Korean J. Chem. Eng., **29**(8), 989-993 (2012)
DOI: 10.1007/s11814-012-0031-2

RAPID COMMUNICATION

A novel and simple approach for the synthesis of Fe_3O_4-graphene composite

Feng-Jun Zhang*,,†, Jin Liu*, Kan Zhang**, Wei Zhao***, Won-Kweon Jang****, and Won-Chun Oh***,†**

*Anhui Key Laboratory of Advanced Building Materials, Anhui University of Architecture, Anhui Hefei 230022, P. R. China
**Engineering Research Center of Building Energy-efficient Control and Evalution, Ministry of Education, Hefei 230022, China
***Department of Advanced Materials Science & Engineering, Hanseo University, Seosan-si, Chungnam 356-706, Korea
****Div. of Electronic, Computer, and Communication Engineering, Hanseo University, Seosan-si, Chungnam 356-706, Korea
(*Received 2 January 2012 • accepted 7 March 2012*)

Abstract−High crystalline Fe_3O_4-graphene composite has been successfully synthesized *via* one-step thermolysis reaction. The results demonstrated that the attachment of iron-organic complex with graphene oxide sheets can facilely lead to magnetic graphene composites with a time-dependent calcination process. The composite was characterized by scanning electron microscopy, transmission electron microscopy, Raman spectroscopy, X-ray diffraction, and X-ray photoelectron spectroscopy. The high efficient removal of methylene blue determined that Fe_3O_4-graphene is a promising sorbent material for wastewater treatment.

Key words: Graphene, Fe_3O_4, Thermolysis Reaction, Removal

INTRODUCTION

Magnetic graphene composites are generally obtained by graphene decorated with magnetic nanoparticles, including Fe [1], FeOH [2], γ-Fe_2O_3 [3] and Fe_3O_4 [4,5] and so on. Among them, Fe_3O_4/graphene composite has long been attractive because it has potential applications in enhanced optical limiting, MRI, drug delivery, Li ion batteries and removal of contaminants from waste water [4,6-9]. Since Chandra et al. reported nearly complete (over 99.9%) arsenic removal using a magnetic graphene in 2010 [10], graphene and its composites have become more and more popular in wastewater purification [11-13]. In particular, the magnetic graphene has absolute advantage for its separation from water. Although the new type of magnetic graphene has shown promising use in treating waste water, its complicated producing procedures and milligram-production-scale still limit its application in backward countries. Hence, it is still a major challenge to develop simple and facile approaches with low costs for the synthesis of magnetic graphene.

However, these complicated synthesis procedures for high crystalline Fe_3O_4/graphene make their impossibility in industrial production and application. Herein, we have synthesized the composite of graphene decorated with high crystalline Fe_3O_4 nanoparticles with a novel and simple thermolysis reaction. Furthermore, taking MB removal as a model, we demonstrated that our Fe_3O_4-graphene composites have really great potential in wastewater treatment.

EXPERIMENT

1. Synthesis of Fe_3O_4-graphene Composite

Graphene oxide (GO) was prepared from natural graphite (KS-6) according to Hummer's method [14]. Fe_3O_4-graphene composite was produced as follows: one gram of the graphene oxide powder was dispersed into 400 mL water-alcohol solution with 1 : 1 volume ratio to yield a homogeneous brown suspension. 3.4 g bis (cyclopentadienyl) iron was then added into the graphene oxide suspension and stirred for 30 min. After physical adsorption, the complex was filtered and dried at 50 °C, and then calcined at 600 °C under an oxygen-free condition for 1 h. After being cooled to room temperature, the Fe_3O_4-graphene composite was obtained.

2. Characterization

XRD patterns were obtained with a diffractometer (Shimata XD-D1, Japan) using Cu Kα radiation. Raman spectra were carried out by a Horiba Jobin Yvon LabRAM using a 100×objective lens with a 532 nm laser excitation. The state of the dispersed Fe_3O_4 on graphene-nanosheets was observed using transmission electron microscopy (TEM, JEOL, JEM-2010, Japan). The clean transparent solution was analyzed by using a UV/Vis spectrophotometer. The spectra for each sample were recorded and the absorbance was determined at characteristic wavelength 660 nm for the each MB solution degraded.

3. Adsorption Ability

5 mg Fe_3O_4-graphene composites were added into 20 mL 0.1 gL^{-1} MB aqueous solution. After 20 s magnetic separation by an external magnetic field under natural lighting, the clean transparent solution was analyzed by a UV/Vis spectrophotometer, and the absorbance at characteristic wavelength 660 nm was determined for each MB solution.

RESULTS AND DISCUSSION

XRD is a rapid analytical technique primarily used for phase identification of crystalline materials and can provide information on unit cell dimensions. Fig. 1 shows the XRD patterns of GO, graphene, Fe_3O_4-graphene calcined for 10 min and 60 min, respectively. It is obvious that the magnetic graphene composite formation is a time-dependent synthesis process. Since GO prepared from graphite by

†To whom correspondence should be addressed.
E-mail: zhang-fengjun@hotmail.com, wc_oh@hanseo.ac.kr

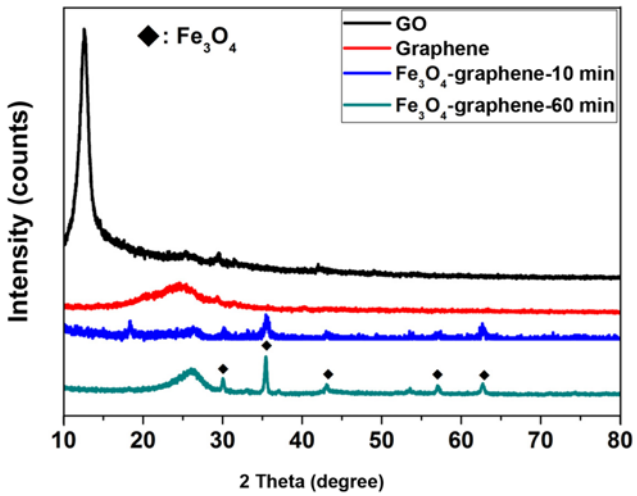

Fig. 1. XRD patterns of GO, graphene, Fe_3O_4-graphene calcined for 10min and 60 min.

liquid-phase oxidation is one of the intercalation compounds, it can be found that the *d*-spacing of GO layers (0.42 nm) is larger than that of the layers of graphite (0.34 nm), as has been mentioned by Lee et al. [15]. At calcining time of 10 min, converting iron complex attached to small magnetite subparticles with weak crystallization is obtained, corresponding to the low-intensity diffraction peaks of magnetite in the XRD pattern, and the crystalline substances with obvious diffraction peaks correspond to GO and graphene at 18.4° and 26.3°, respectively [10]. With the calcining time up to 60 min, these unstable subparticles with high surface energy tend to aggregate and grow into high crystalline magnetite nanoparticles by van der Waals forces and magnetic dipole [4], while a rising peak can index to graphene phase which is further shifted into high 2θ degree compared to pristine graphene. Because GO has many defects or nanoholes, it is reasonable that thermally reduced graphene would also have many defects and nanoholes (d_{Df}). Therefore, GO and graphene can have oxide groups of C-Ox with some sp3 bonds in their defects and nanoholes (d_{Ox}). GO has the largest interlayer distance (d_{GO}) because of its intercalated H_2O molecules and various oxide groups. If defects in the layer are sufficiently large, oxide groups and H_2O molecules can be considered to exist in the empty space. On the basis of a model with various interlayers, it can be inferred that GO has an intermediate structure with d_{Ox} and d_{Df} during thermal reduction, and through bottom-up layer stacking, the resultant graphene evolves toward graphite as crystal growth with the removal of d_{Ox} and d_{Df} [16]. However, the prior formation of iron-organic complex onto GO surface by chemical interaction will reduce the removal of d_{Ox} and d_{Df}, so that the XRD pattern of Fe_3O_4-graphene displays a rising peak at high 2θ degree compared to pristine graphene.

The time-dependent crystal growth was further investigated by TEM. As shown in Fig. 2(a), the Fe_3O_4-graphene composite after calcination for 10 min shows that the small magnetite subparticles were attached onto graphene surface. With calcining up to 60 min, these subparticles gradually grew to high crystalline Fe_3O_4 nano-

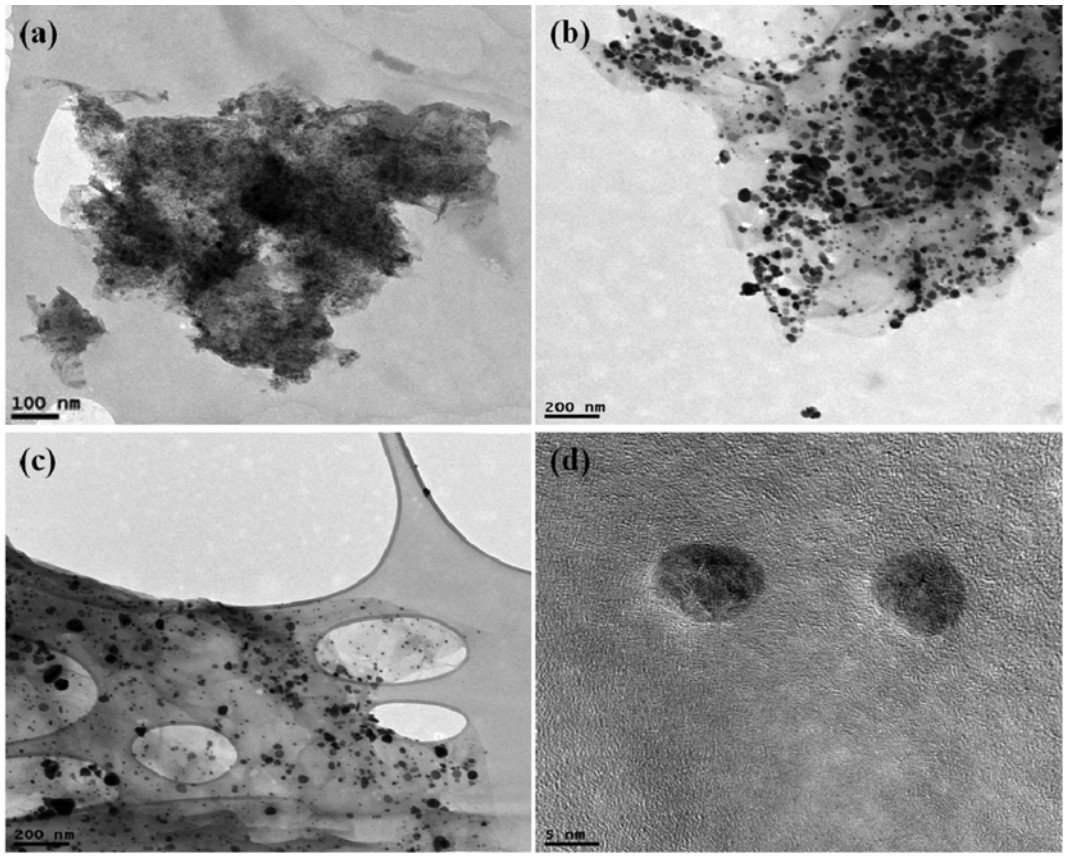

Fig. 2. TEM images of Fe_3O_4-graphene calcined for 10 min (a) and 60 min (b)-(c). HR-TEM image of Fe_3O_4-graphene calcined for 60 min (d).

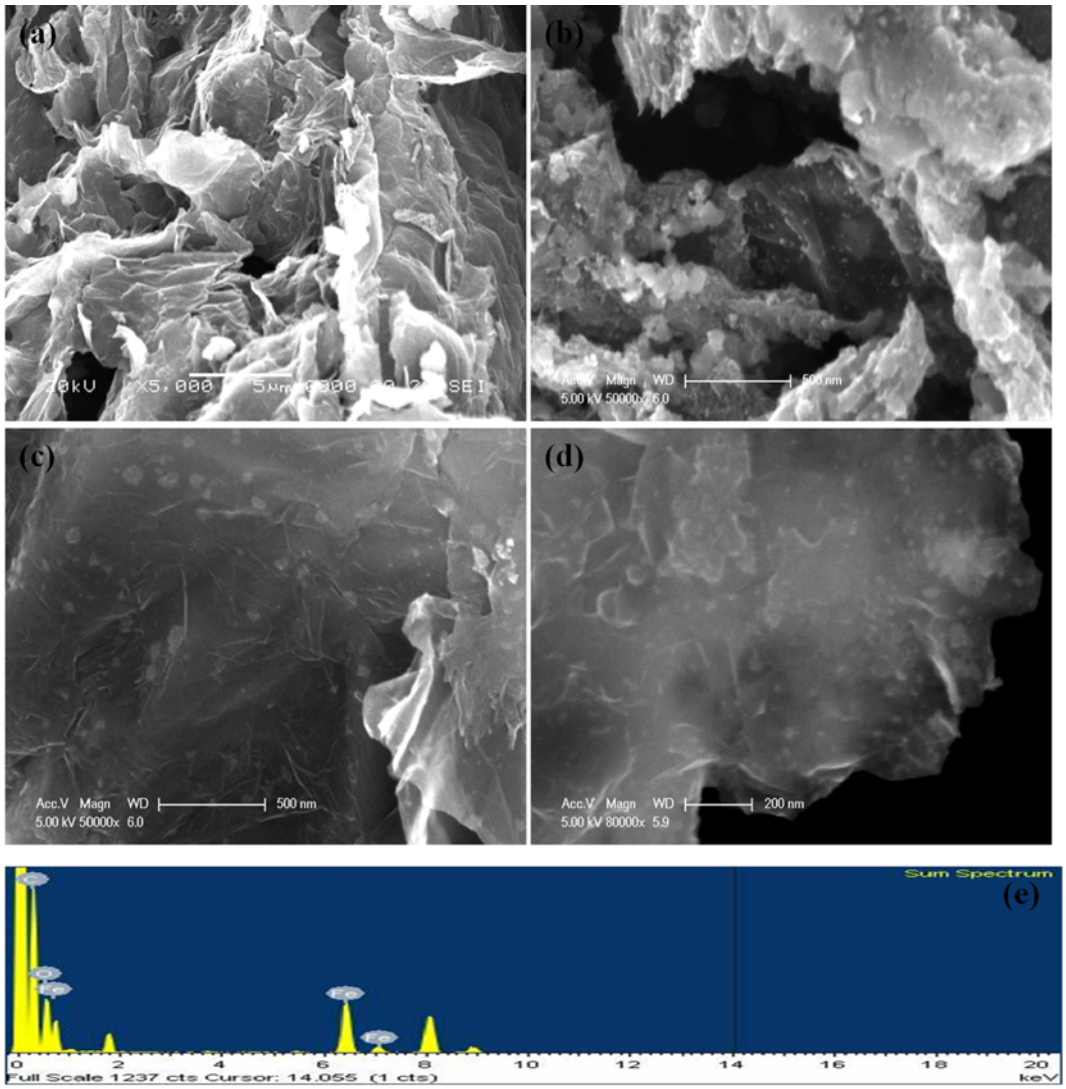

Fig. 3. SEM images of (c) graphene, and (b)-(d) Fe_3O_4-graphene. (e) EDX spectrum of Fe_3O_4-graphene.

particles by high temperature thermolysis (Fig. 2(b)-(c)). The size of the Fe_3O_4 nanoparticles was found to be below 10 nm, as measured in Fig. 2(d). The microstructure of the Fe_3O_4-graphene composite was characterized by SEM. In the case of graphene, because of oxidation and heat treatment, it broke into pieces smaller than pristine graphite, as observed in Fig. 3(a). The SEM images taken from graphene and Fe_3O_4-graphene composites (Fig. 2(b)-(d)) showed that they possessed a layer-by-layer assembled structure consisting of graphene nanosheets and Fe_3O_4 particles. These results could be further confirmed by EDX spectrum (Fig. 3(e)).

Fig. 4(a) shows the Raman spectra of GO and Fe_3O_4-graphene. Peaks of GO at 1,592 cm^{-1} and 1,350 cm^{-1} correspond to sp^2 carbon domains (G band) and sp^3 (D band) hybridization inducing defects, respectively [17]. Compared with GO, the ratio of intensities (I_D/I_G) for Fe_3O_4-graphene samples has a remarkable increase, and the G mode of Fe_3O_4-graphene becomes weaker and broader, suggesting a higher level of disorder of the graphene layers due to deoxygenation and introduction of Fe_3O_4 during high temperature thermolysis [18]. Fig. 4(b) shows the XPS patterns of the GO and Fe_3O_4-graphene. The peaks $Fe2p_{3/2}$ and $Fe2p_{1/2}$ are located at ~712 and ~724 eV, respectively, and not at ~710 eV which is for γ-Fe_2O_3 [19]. This indicates the formation of the Fe_3O_4 phase in the graphene matrix [20]. In addition, a decrease of O/C ratio with calcining time indicates a considerable reduction of GO.

The Fe_3O_4-graphene composite combines the high adsorption capacity of graphene and the separation convenience of magnetic nanoparticles, which makes it an excellent candidate for the removal of contaminants from water. As determined in Fig. 5(a), the BET specific surface area of Fe_3O_4-graphene composite is 41 m^2/g. The relatively large specific surface area is beneficial for effective absorbent for removing contaminants in water. As shown in the top left inset of Fig. 5(b), after dispersing of Fe_3O_4-graphene composites in the MB solution and shaking the resultant mixture by hand for only 1 minute under natural lighting, the magnetic graphene nanosheets could be easily separated from the mixture by an external magnetic field and the solution became colorless. It can be considered that high sensitivity to the external magnetic field could be remarkably enhanced by decorating graphene sheets with magnetic Fe_3O_4 nanoparticles [21]. The UV spectra show nearly complete MB removal from water (Fig. 4(b)).

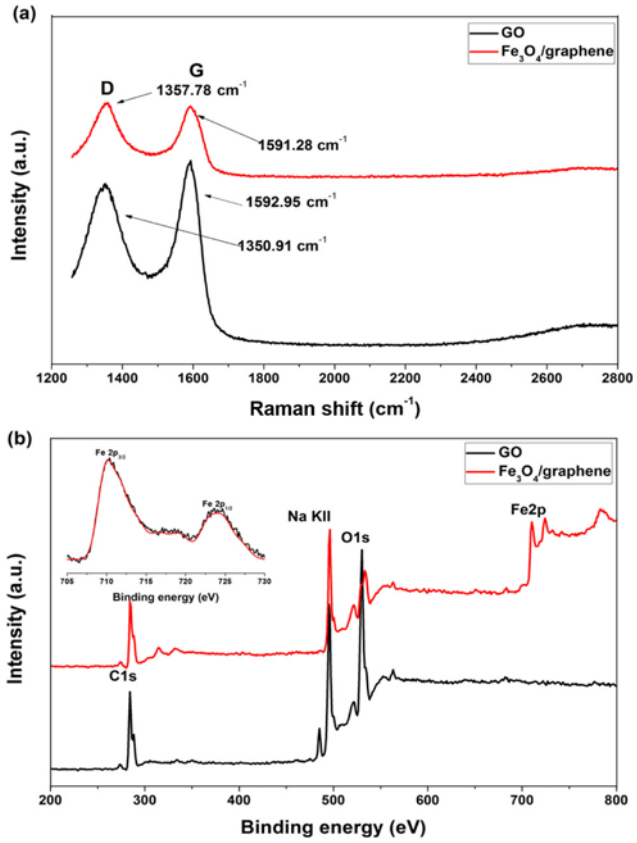

Fig. 4. Raman (a) and XPS (b) spectra of graphene and Fe_3O_4-graphene.

The advantages of Fe_3O_4-graphene composite for removal of MB from solution are investigated by comparing pure graphene and Fe_3O_4, as shown in Fig. 5. Graphene sheets were removed from the MB solution by centrifugation. Fe_3O_4-graphene and Fe_3O_4 were removed from the MB solution by an external magnetic field. The data for adsorption of MB dye by different samples were measured at the same time intervals. The results show that the Fe_3O_4-graphene composite has fast adsorption kinetics towards MB dye solution within 20 min.

Finally, according to most of the synthetic approaches of magnetic graphene documented so far, the thermolysis reaction mechanism for producing this material is still unclear. Despite many previously reported analogous cases in which magnetic graphene has been completed using organic compound by a hydrothermal method, the resulting composite usually has a mixed (γ-Fe_2O_3+Fe_3O_4) phase [3,22]. Although other researchers have used organic salt as the reaction initiator for synthesizing high crystalline Fe_3O_4-graphene, the reaction process still takes a long time [5,23,24]. The proposed mechanism for the synthesis is tentatively explained as follows: 1) the ferrocene can be attached onto GO surface through physical adsorption, electrostatic binding or charge transfer [25]. 2) At high temperature, GO is deoxygenated [26], the product being mainly CO_2 and H_2O. 3) Because ferrocene is well soluble in Sc-CO_2 [27] at a temperature higher than that of thermolysis, the low valence iron cations in ferrocene were slowly oxidized by CO_2, substituting the cyclopentadienyl-group and oxidizing Fe^{2+} to high crystalline Fe_3O_4.

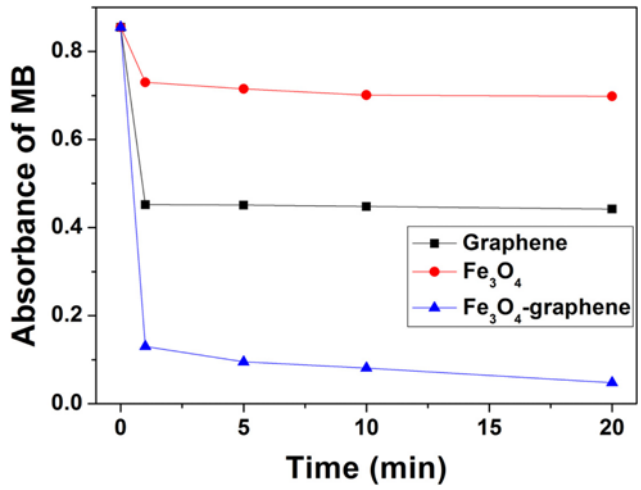

Fig. 6. Kinetic adsorption data plots for MB.

CONCLUSION

We successfully synthesized high crystalline Fe_3O_4-graphene composites *via* a time-dependent thermolysis reaction, where high crystalline Fe_3O_4 nanoparticles are hybrided with graphene nanosheets. With

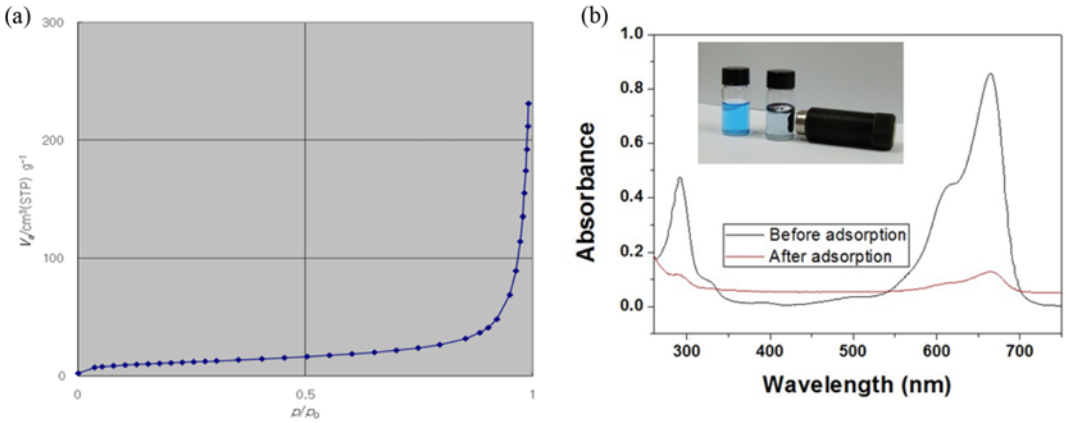

Fig. 5. N_2 adsorption isotherms of Fe_3O_4-graphene composite (a). Uv-Vis spectra of MB solution before and after adsorption by Fe_3O_4-graphene (b). The inset in Fig. 4(b) shows the adsorption process of Fe_3O_4-graphene for MB.

the development of the preparation technology of Fe_3O_4-graphene, the simple procedure not only contributed to the cost of Fe_3O_4-graphene, but also provided high crystalline of Fe_3O_4-graphene for more applications in the near future. This paper is relevant and important for the application of a magnetic separation method and graphene in environmental pollution cleanup.

ACKNOWLEDGEMENT

The authors thank for financial supports from the Doctor Foundation (2011), Open Foundation of Building Energy-saving Institute (Grant No. 2012-08) and College Students' Science and Technology Innovation Foundation of Anhui University of Architecture (2011).

REFERENCES

1. H. Jabeen, V. Chandra, S. H. Jung, J. W. Lee, K. S. Kim and S. B. Kim, *Nanoscale*., **3**, 3583 (2011).
2. K. Zhang, V. Dwivedi, C. Y. Chi and J. S. Wu, *J. Hazard. Mater*., **182**, 162 (2010).
3. J. F. Shen, Y. Z. Hu, M. Shi, N. Li, H. W. Ma and M. X. Ye, *J. Phys. Chem. C*., **114**, 1498 (2010).
4. H. P. Cong, J. J. He, Y. Lu and S. H. Yu, *Small*., **6**, 169 (2010).
5. X. P. Shen, J. L. Wu, S. Bai and H. Zhou, *J. Alloys. Compd*., **506**, 136 (2010).
6. X. Y. Zhang, X. Y. Yang, Y. F. Ma, Y. Huang and Y. S. Chen, *J. Nanosci. Nanotechnol*., **10**, 2984 (2010).
7. G. M. Zhou, D. W. Wang, F. Li, L. L. Zhang, N. Li, Z. S. Wu, L. Wen, G. Q. Lu and H. M. Cheng, *Chem. Mater*., **22**, 5306 (2010).
8. X. Y. Yang, X. Y. Zhang, Y. F. Ma, Y. Huang, Y. S. Wang and Y. S. Chen, *J. Mater. Chem*., **19**, 2710 (2009).
9. F. He, J. T. Fan, D. Ma, L. M. Zhang, C. Leung and H. L. Chan, *Carbon*., **48**, 3139 (2010).
10. V. Chandra, J. S. Park, Y. Chun, J. W. Lee, I. C. Hwang and K. S. Kim, *ACS Nano*., **4**, 3979 (2010).
11. V. Chandra and K. S. Kim, *Chem. Commun*., **47**, 3942 (2011).
12. X. J. Deng, L. L. Lv, H. W. Li and F. Luo, *J. Hazard. Mater*., **183**, 923 (2010).
13. H. M. Sun, L. Y. Cao and L. H. Lu, *Nano. Res*., **4**, 550 (2011).
14. W. S. Hummers and R. E. Offeman, *J. Am. Chem. Soc*., **80**, 1339 (1958).
15. S. H. Lee, H. W. Kim, J. O. Hwang, W. J. Lee, J. Kwon, C. W. Bielawski, R. S. Ruoff and S. O. Kim, *Angew. Chem. Int. Ed*., **49**, 10084 (2010).
16. H. M. Ju, S. H. Choi and S. H. Huh, *J. Kor. Phys. Soc*., **57**, 1649 (2010).
17. F. Tuinstra and J. L. Koenig, *J. Chem. Phys*., **53**, 1126 (1970).
18. A. C. Ferrari and J. Robertson, *Phys. Rev. B*., **61**, 14095 (2000).
19. J. Lu, X. Jiao, D. Chen and W. Li, *J. Phys. Chem. C*., **113**, 4012 (2009).
20. D. Zhang, Z. Liu, S. Han, C. Li, B. Lei, M. P. Stewart, J. M. Tour and C. Zhou, *Nano. Lett*., **4**, 2151 (2004).
21. J. E. Kim, T. H. Han, S. H. Lee, J. Y. Kim, C. W. Ahn, J. M. Yun and S. O. Kim, *Angew. Chem. Int. Ed*., **50**, 3043 (2011).
22. J. F. Shen, M. Shi, H. W. Ma, B. Yan, N. Li and M. X. Ye, *Mater. Res. Bull*., **46**, 2077 (2011).
23. X. Y. Li, X. L. Huang, D. P. Liu, X. Wang, S. Y. Song, L. Zhou, H. J. Zhang, *J. Phys. Chem. C*., **115**, 21567 (2011).
24. Y. Zhang, B. Chen, L. M. Zhang, J. Huang, F. H. Chen, Z. P. Yang, J. L. Yao and Z. J. Zhang, *Nanoscale*., **3**, 1446 (2011).
25. G. Williams, B. Seger and P. V. Kamat, *ACS Nano*., **2**, 1487 (2008).
26. D. X. Yang, A. Velamakanni, G. Bozoklu, S. J. Park, M. Stoller, R. D. Piner, S. Stankovich, I. H. Jung, D. A. Field, C. A. Ventrice Jr. and R. S. Ruoff, *Carbon*., **47**, 145 (2009).
27. C. M. Cowey, K. D. Bartle, M. D. Burford, A. A. Clifford and S. Zhu, *J. Chem. Eng. Data*., **406**, 1217 (1995).